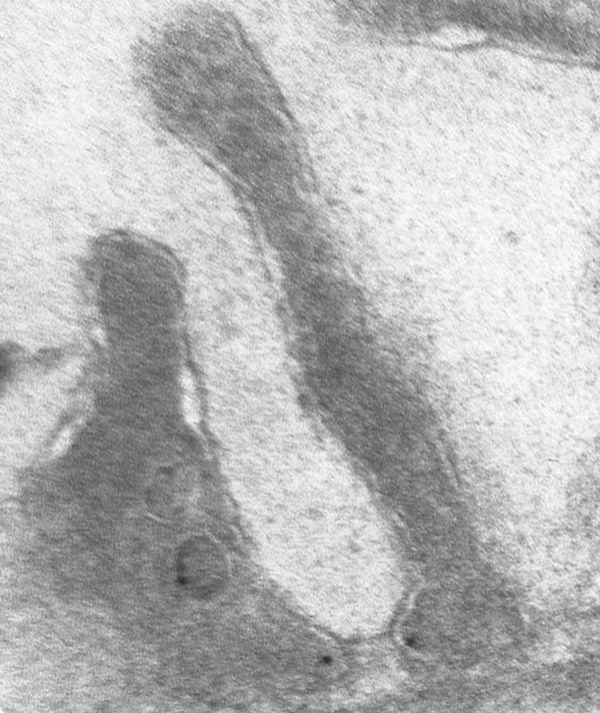

Supplemental Figure 1. Pod-*Dnm*-DKO mice have characteristic lesions suggestive of focal segmental glomerulosclerosis.

(A) E 16.5 isolated podocytes immunoblotted with anti-dynamin1 and 2, and anti-WT1 antibodies as control demonstrates residual expression at this early age. (B) Lower weight gain in pod-*Dnm*-DKO mice relative to controls after 4 weeks of age. (C) At 8 weeks, pod-*Dnm*-DKO mice have a dramatically reduced kidney to body weight ratio *$p<0.01$ N=4. (D) Kidneys of pod-*Dnm*-DKO mice are paler and smaller than controls and have a corrugated appearance. (E) Representative light microscopy images (H and E, PAS, and Trichrome) of glomeruli from pod-*Dnm*-DKO mice revealing histological evidence of focal segmental glomerulosclerosis at 4 weeks of age which progresses to global sclerosis at 10 weeks. Scale Bar 25μm. (F) Proteinaceous casts, dilated tubules, and interstitial fibrosis in Pod-*Dnm*-DKO at 6 and10 weeks Scale Bar 50μm.

Supplemental Figure 2. Albumin and Creatinine quantification in Pod-*Dnm*-DKO, *Synj1* KO and *endophilin* TKO mice.

(A-D) Individual dot blots of measured albumin and creatinine for wild type and above mutant mice.

Supplemental Figure 3. Mice lacking dynamin, synaptojanin 1, and or endophilin have foot process effacement and wild type podocytes have numerous clathrin coated pit intermediates.

(A) Quantification of foot processes per micrometer of glomerular basement membrane from indicated mice *,**,***$p<0.001$. (B) Representative electron microscopy images of clathrin coated pits in wild type podocytes. Scale Bar 200nm.

Supplemental Figure 4. Kidneys from *Synj1* KO mice have glomerular defects and elevated PI(4,5)P2 levels.

(A) Representative images of H and E, PAS, and trichrome stained glomeruli from *Synj1* KO mice and littermate controls. Scale Bar 25μm. Squares indicate mesangial accumulation. (B) Representative low power images of H and E, PAS, and trichrome stained kidney sections from *Synj1* KO mice and littermate controls. Scale Bar 25μm. Note proteinaceous casts in *Synj1* KO mice indicated by an arrowhead. (C) *Synj1* KO kidneys have elevated PI(4,5)P2 levels. *$p<0.05$ N=4. (D) EM image from E16.5 *Synj1* KO mice demonstrates foot process effacement. Scale Bar 500 nm.

Supplemental Figure 5. Endophilin TKO kidneys demonstrate mesangial matrix accumulation.

(A) Representative images of H and E, PAS, and trichrome stained glomeruli from *endophilin* TKO mice and littermate controls. Scale Bar 25μm. Squares indicate mesangial accumulation .(B) Representative low power images of H and E, PAS, and trichrome stained kidney sections from *endophilin* TKO mice and littermate controls. Scale Bar 25μm. Note the proteinaceous casts in *endophilin* TKO mice (indicated by arrowheads).

Supplemental Figure 6. Dynamin 2 and synaptojanin 1 colocalize with clathrin in podocytes.

(A) Presence of Dynamin2-GFP at a subset of clathrin coated pits as detected by colocalization with mRFP-CLC (selected examples highlighted by arrowheads). Scale Bar 2.5 μm (B) Selected

frames from a time series of a clathrin coated pit acquired from time 0-170 sec. Merged images (bottom) demonstrate late arrival of dynamin at clathrin coated pits just before membrane fission and clathrin coated pit disappearance from the plane of imaging. (C) Lifetime distribution of dynamin *2* and mRFP-CLC. (D) Colocalization of clathrin (mRFP-CLC) and GFP-Synaptojanin 1. Arrowheads highlight selected examples. Scale Bar 2.5μm. (E) Selected frames from a time series of a clathrin coated pit acquired from time 0-168 sec. Note that Synaptojanin 1 is already present at early stage clathrin coated pits from time. (F) Lifetime distribution of mRFP-CLC and GFP-Synaptojanin 1 taken from time-lapse video microscopy. (G) Robust accumulation of endophilin 2 from Pod-Dnm-DKO podocytes. Scale Bar 20μm.

Supplemental Figure 7. Relative clathrin coated pit recruitment as a function of time for selected pairs of proteins.

(A) Fluorescence intensity as a function of time for dynamin 2 and utrophin, which appear and disappear together. (B) Fluorescence intensity as a function of time for synaptojanin 1 and utrophin demonstrates presence of utrophin coinciding with the disappearance of synaptojanin 1. (C) Fluorescence intensity as a function of time for endophilin 2 and utrophin which appear and disappear in at similar time points. (D) Fluorescence intensity as a function of time for endophilin 2 and clathrin. Endophilin 2 arrives prior to pit disappearance. (E) Fluorescence intensity as a function of time for Myo1e and clathrin. Myosin 1E arrives just prior to pit disappearance. (F) Fluorescence intensity as a function of time for Myosin 1E and utrophin which appear and disappear together. (G) Relative fluorescence intensity as a function of time for CD2AP and clathrin demonstrating late arrival of CD2AP at pits just prior to the disappearance of clathrin.

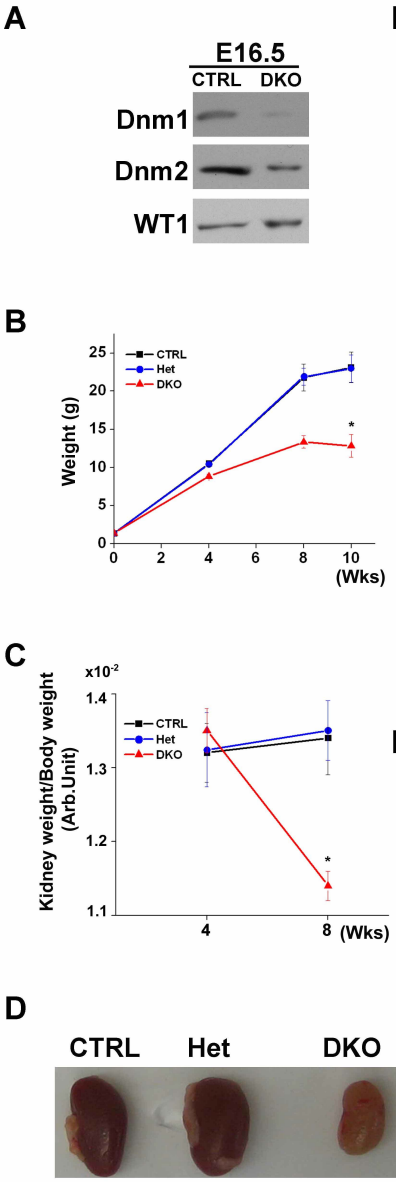

Supplemental Figure 1. Pod-*Dnm*-DKO mice have characteristic lesions suggestive of focal segmental glomerulosclerosis. (A) E 16.5 isolated podocytes immunoblotted with anti-dynamin1 and 2, and anti-WT1 antibodies as control demonstrates residual expression at this early age. (B) Lower weight gain in pod-*Dnm*-DKO mice relative to controls after 4 weeks of age. (C) At 8 weeks, pod-*Dnm*-DKO mice have a dramatically reduced kidney to body weight ratio *p<0.01 N=4. (D) Kidneys of pod-*Dnm*-DKO mice are paler and smaller than controls and have a corrugated appearance. (E) Representative light microscopy images (H and E, PAS, and Trichrome) of glomeruli from pod-*Dnm*-DKO mice revealing histological evidence of focal segmental glomerulosclerosis at 4 weeks of age which progresses to global sclerosis at 10 weeks. Scale Bar 25μm. (F) Proteinaceous casts, dilated tubules, and interstitial fibrosis in Pod-*Dnm*-DKO at 6 and10 weeks Scale Bar 50μm.

Supplemental Fig 1

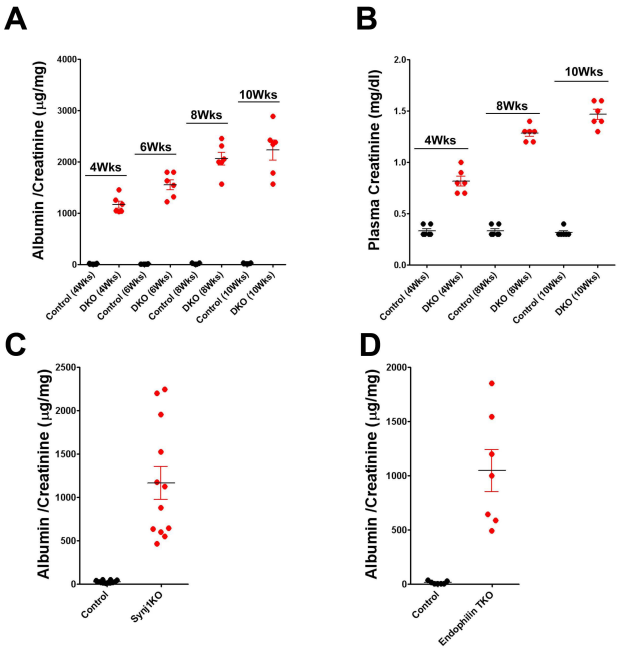

Supplemental Figure 2. Albumin and Creatinine quantification in Pod-*Dnm*-DKO, *Synj1* KO and *endophilin* TKO mice.

(A-D) Individual dot blots of measured albumin and creatinine for wild type and above mutant mice.

Supplemental Fig 2

A

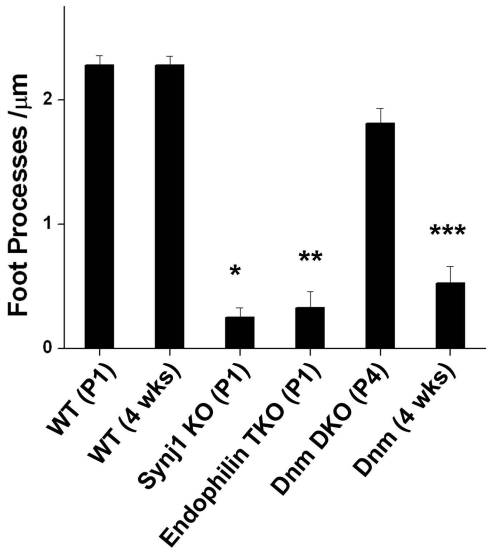

Supplemental Figure 3. Mice lacking dynamin, synaptojanin 1, and or endophilin have foot process effacement and wild type podocytes have numerous clathrin coated pit intermediates.
(A) Quantification of foot processes per micrometer of glomerular basement membrane from indicated mice *,**,***p<0.001. (B) Representative electron microscopy images of clathrin coated pits in wild type podocytes. Scale Bar 200nm.

B

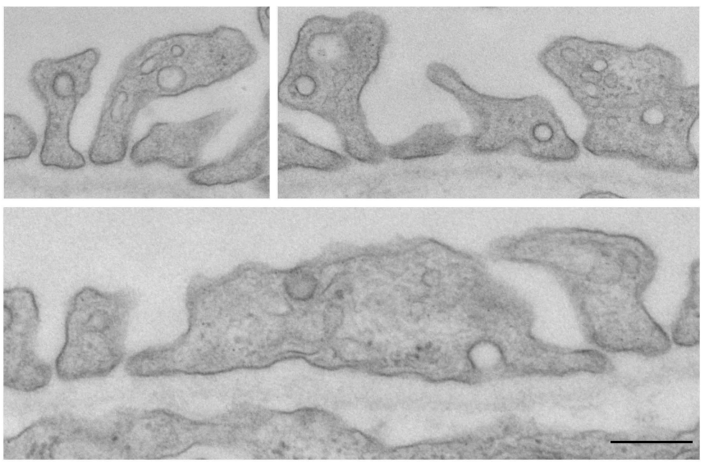

Supplemental Fig 3

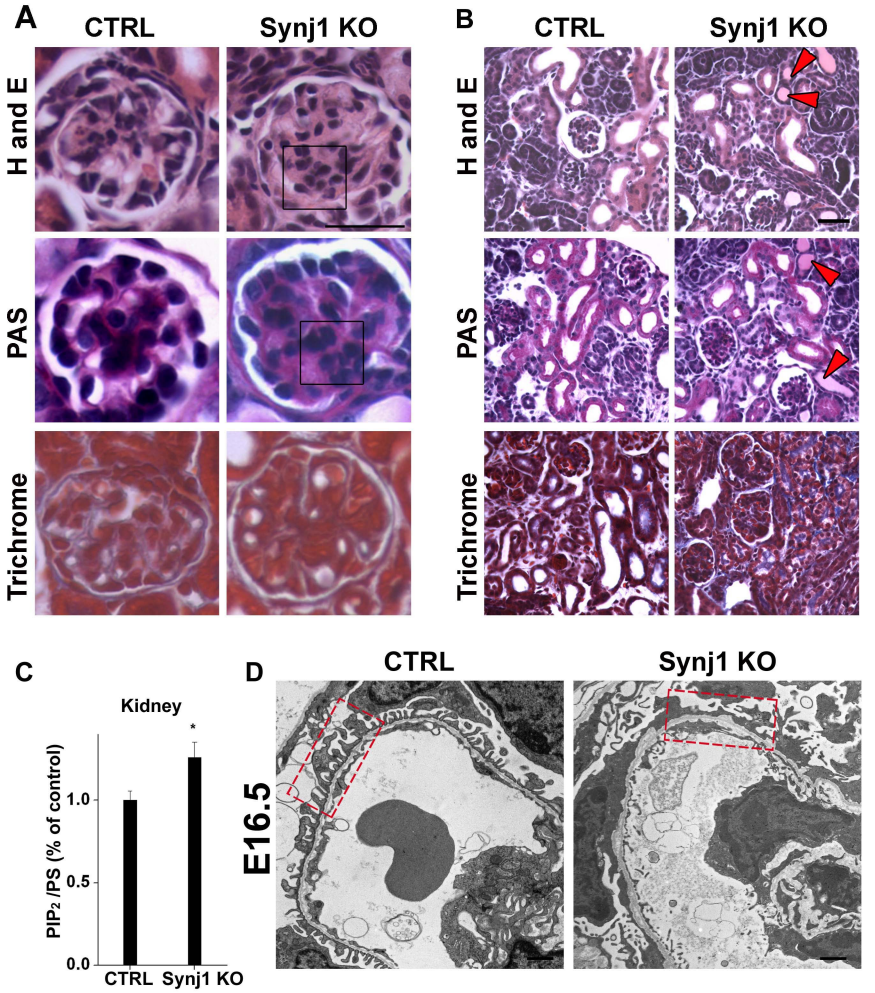

Supplemental Figure 4. Kidneys from *Synj1* KO mice have glomerular defects and elevated PI(4,5)P2 levels.
(A) Representative images of H and E, PAS, and trichrome stained glomeruli from *Synj1* KO mice and littermate controls. Scale Bar 25μm. Squares indicate mesangial accumulation. (B) Representative low power images of H and E, PAS, and trichrome stained kidney sections from *Synj1* KO mice and littermate controls. Scale Bar 25μm. Note proteinaceous casts in *Synj1* KO mice indicated by an arrowhead. (C) *Synj1* KO kidneys have elevated PI(4,5)P2 levels. *p<0.05 N=4. (D) EM image from E16.5 *Synj1* KO mice demonstrates foot process effacement. Scale Bar 500 nm.

Supplemental Fig 4

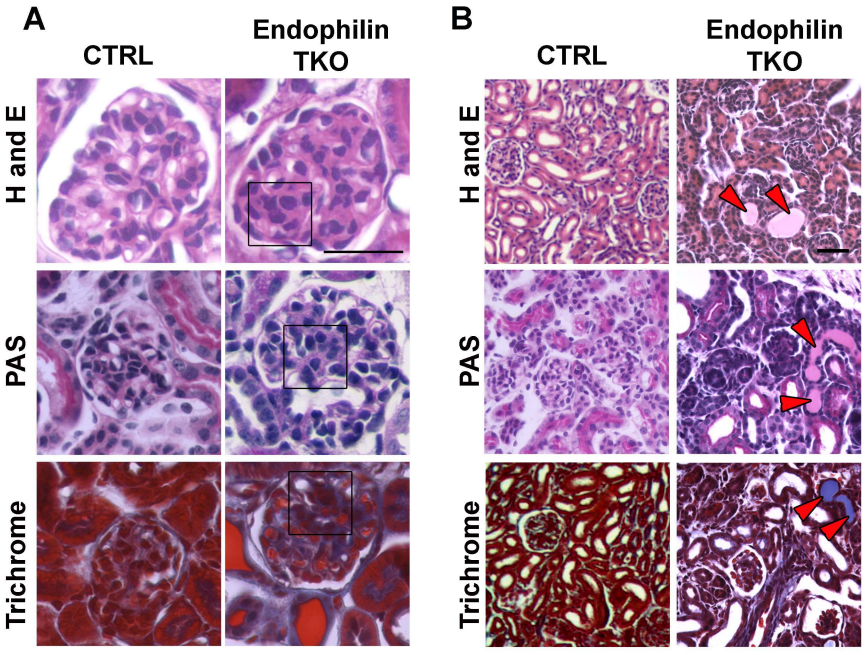

Supplemental Figure 5. Endophilin TKO kidneys demonstrate mesangial matrix accumulation.
(A) Representative images of H and E, PAS, and trichrome stained glomeruli from *endophilin* TKO mice and littermate controls. Scale Bar 25µm. Squares indicate mesangial accumulation .(B) Representative low power images of H and E, PAS, and trichrome stained kidney sections from *endophilin* TKO mice and littermate controls. Scale Bar 25µm. Note the proteinaceous casts in *endophilin* TKO mice (indicated by arrowheads).

Supplemental Fig 5

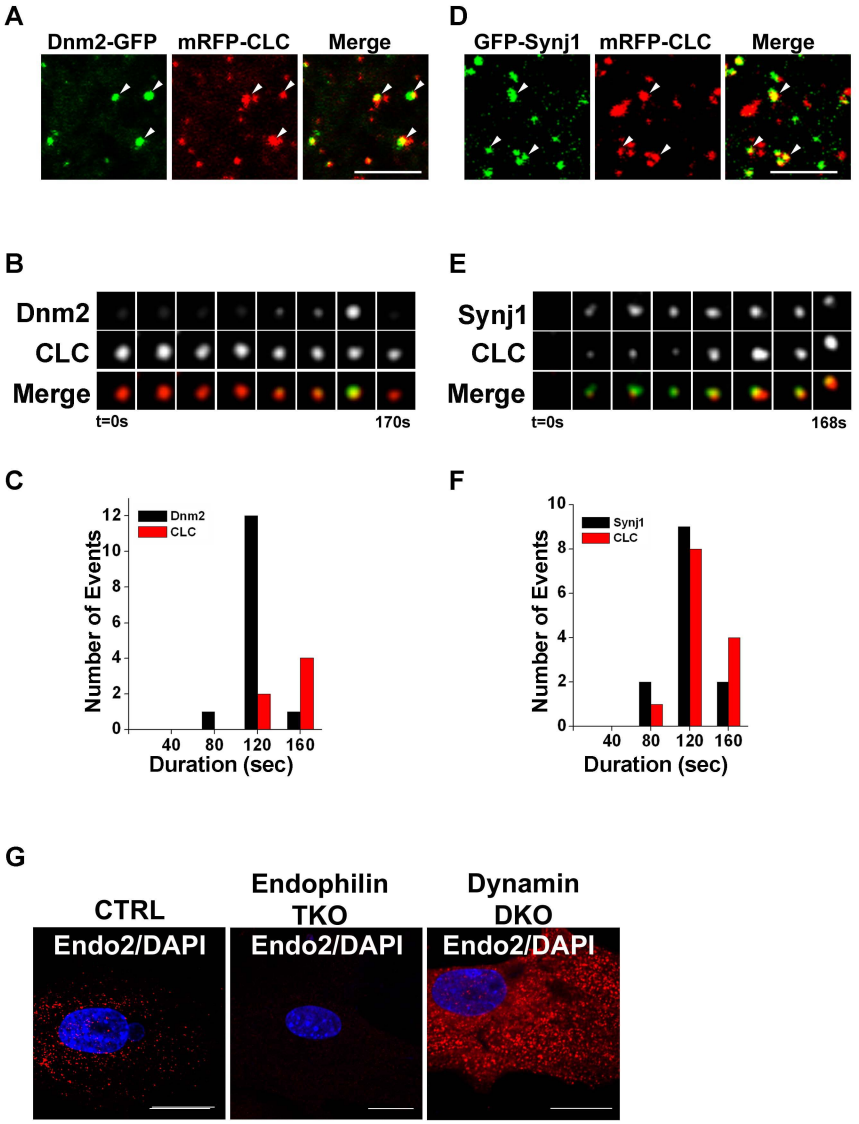

Supplemental Figure 6. Dynamin 2 and synaptojanin 1 colocalize with clathrin in podocytes.

(A) Presence of Dynamin2-GFP at a subset of clathrin coated pits as detected by colocalization with mRFP-CLC (selected examples highlighted by arrowheads). Scale Bar 2.5 μm (B) Selected frames from a time series of a clathrin coated pit acquired from time 0-170 sec. Merged images (bottom) demonstrate late arrival of dynamin at clathrin coated pits just before membrane fission and clathrin coated pit disappearance from the plane of imaging. (C) Lifetime distribution of dynamin *2* and mRFP-CLC. (D) Colocalization of clathrin (mRFP-CLC) and GFP-Synaptojanin 1. Arrowheads highlight selected examples. Scale Bar 2.5μm. (E) Selected frames from a time series of a clathrin coated pit acquired from time 0-168 sec. Note that Synaptojanin 1 is already present at early stage clathrin coated pits from time. (F) Lifetime distribution of mRFP-CLC and GFP-Synaptojanin 1 taken from time-lapse video microscopy. (G) Robust accumulation of endophilin 2 from Pod-Dnm-DKO podocytes. Scale Bar 20μm.

Supplemental Fig 6

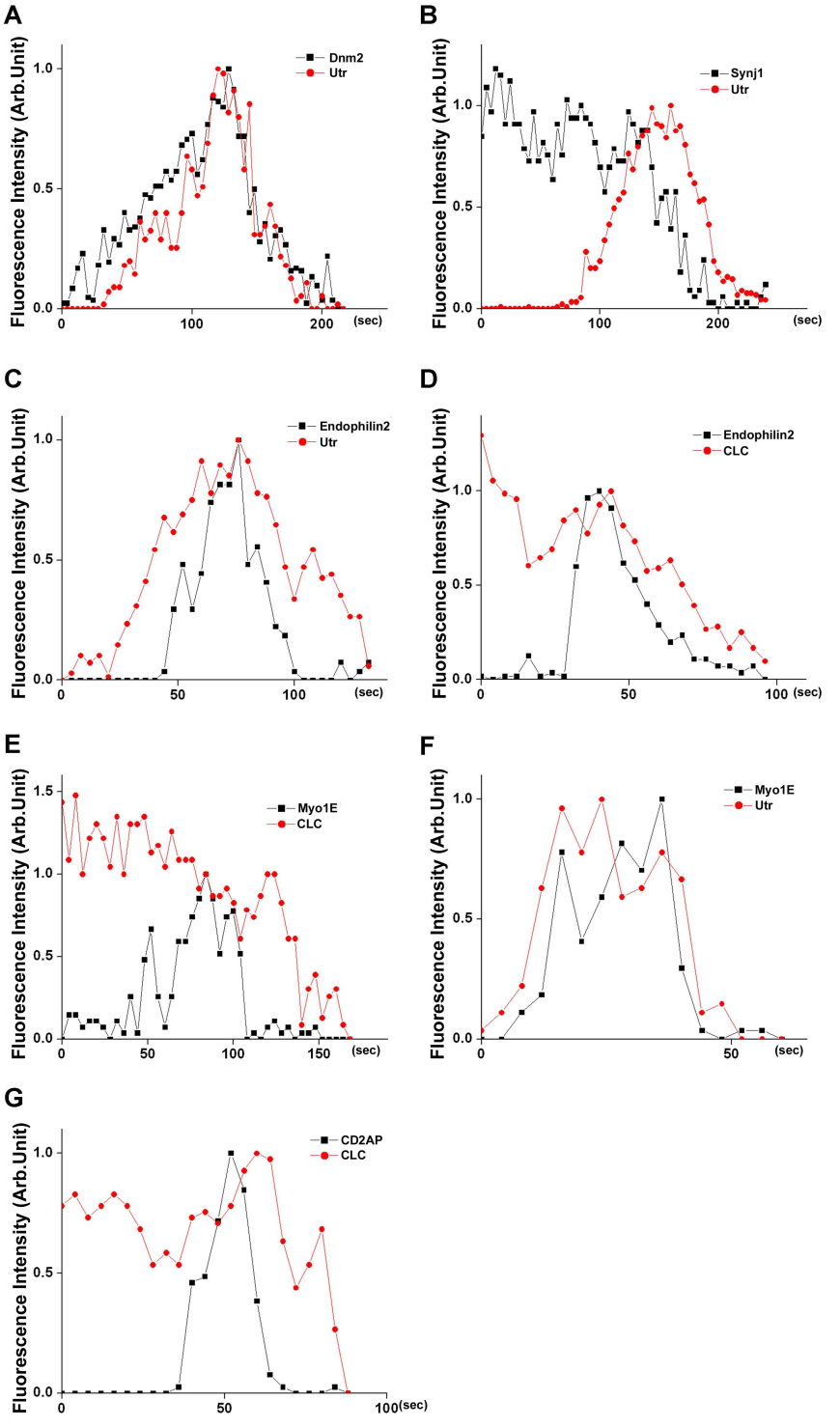

Supplemental Figure 7. Relative clathrin coated pit recruitment as a function of time for selected pairs of proteins. (A) Fluorescence intensity as a function of time for dynamin 2 and utrophin, which appear and disappear together. (B) Fluorescence intensity as a function of time for synaptojanin 1 and utrophin demonstrates presence of utrophin coinciding with the disappearance of synaptojanin 1. (C) Fluorescence intensity as a function of time for endophilin 2 and utrophin which appear and disappear in at similar time points. (D) Fluorescence intensity as a function of time for endophilin 2 and clathrin. Endophilin 2 arrives prior to pit disappearance. (E) Fluorescence intensity as a function of time for Myo1e and clathrin. Myosin 1E arrives just prior to pit disappearance. (F) Fluorescence intensity as a function of time for Myosin 1E and utrophin which appear and disappear together. (G) Relative fluorescence intensity as a function of time for CD2AP and clathrin demonstrating late arrival of CD2AP at pits just prior to the disappearance of clathrin.

Supplemental Fig 7